Elastoplastic Constitutive Model Describing Dilatancy Behavior of Overconsolidated Clay

Zheng Wan[1]; Chenchen Song[2]; Songtao Xue[3]; and Liyu Xie[4]

Abstract: Overconsolidated (OC) clay has a strong dilatancy property, which has a significant effect on ultimate strength and deformation. Compared with normal consolidated (NC) clay, OC clay tends to show a higher strength–stress ratio, lower shear shrinkage, and larger dilatancy, as well as strain hardening and softening. A unified hardening (UH) model is a simple and practical model to describe the stress–strain relationship of OC soil. However, the degree of overconsolidation has a direct effect on dilatancy, which is mainly demonstrated by: (1) the degree of overconsolidation is directly related to the phase transformation stress ratio (M_c) that corresponds to the occurrence of dilatancy. The greater the degree of overconsolidation, the smaller the M_c; and (2) the greater the degree of overconsolidation, the smaller the volume shrinkage strain and the larger the volume dilatancy strain. In a UH model, the stress ratio (η) of the phase transformation is a constant and its value is simplified to be equal to the stress ratio of the critical state (M). A UH model cannot be employed to reflect the fact that the M_c varies with the degree of overconsolidation. To overcome the previous problems, the M_c in the dilatancy equation will be expressed as a power function of the overconsolidation stress ratio parameter (R). To reflect the characteristics of large volume shear shrinkage of underconsolidated (UC) soil, the nonassociative flow rule will be adopted, and the shape of the yield surface modified by state parameters is a water drop surface and the plastic potential surface is an elliptic surface. The improved model could better reflect the double influence of the degree of overconsolidation on dilatancy characteristics. **DOI: 10.1061/(ASCE)GM.1943-5622.0001947**.

Author keywords: Overconsolidated clay; Strength; Deformation; Underconsolidated soils; Dilatancy.

Introduction

Clay in a natural sedimentation site has essentially overconsolidation features (Banerjee and Yousif 1986). Many tests had shown that the dilatancy is the basic deformation behavior for both sand and clay (Reynolds 1885; Rowe 1962; Matsuoka and Sakakibara 1987; Oda and Konishi 1974). The degree of overconsolidation has been adopted to measure the maximum stress that the clay unit has ever experienced during its stress history. A large number of laboratory tests have confirmed that the greater the degree of overconsolidation, the smaller the volume shear shrinkage, and the larger the volume dilatancy under shear loading. In addition, with the increase of overconsolidation degree, dilatancy is more probable to occur; therefore, the stress ratio (η) from shear shrinkage to dilatancy will be smaller. Some heavy overconsolidation degree clays even produce dilatancy directly under shear loading. Dilatancy has two effects on overconsolidated (OC) clay; the first is the change rule of volume change and the final volume variable, and the second is the contribution to the strength of OC clay. The larger the overconsolidation degrees, the smaller the volume shrinkage and the larger the volume dilatancy (Ling et al. 2002; Roscoe et al. 1963; Asaoka 2004; Wood 1990; Casagrande and Carillo 1944; Ohta and Nishihara 1985; Whittle 1993; Wood and Graham 1990). In addition, with the increase in the overconsolidation degree, volume dilatancy occurs more easily, which means a lower η that correspond to the transformation phase from the volume shrinkage to the dilatancy will be generated. For some heavy OC clays, dilatancy occurs without shrinkage under shear loading. Dilatancy has two effects on the OC clay: (1) it influences the change law of volume strain and the final volume strain; and (2) it contributes to the strength of OC clay. Test results have demonstrated that the dilatancy volume for heavy OC soil is considerable. Under undrained conditions, it leads to the negative pressure and effective stress increasing further. The η is always above the critical state line (CSL) and eventually gradually approaches the CSL during the loading process or reaches a point above the CSL. When η crosses the peak point, the increment of dilatancy decreases gradually. As η tends to the critical state stress ratio (M), the dilatancy increment tends to zero. For underconsolidated (UC) soils, due to their failure to undergo a normal consolidation process, a larger volume compaction characteristic is shown during the isotropic loading test (Rouainia and Wood 2000; Jovicic and Coop 1998; Simith et al. 1992), but the critical state characteristics are the same as those of the NC clay. During the simulation of clay, the modified Cam-Clay (MCC) model, which is based on the normal consolidation remodeling clay test result, is the most universal elastoplastic constitutive model. When η is maintained at zero, which means isotropic compression and η is maintained at M, the MCC model accurately describes the volume compression characteristics for the previous conditions. Therefore, the interpolation function can be employed to describe the volume change behavior for η between the previous two examples. The dilatancy equation employed in the MCC model can be expressed as

$$\frac{d\varepsilon_v^p}{d\varepsilon_d^p} = \frac{M^2 - \eta^2}{2\eta} \tag{1}$$

[1]Associate Researcher, Research Institute of Base and Foundation, China Academy of Building Research, Beijing 100013, China (corresponding author). Email: zhengw111@126.com

[2]Engineer, China State Construction Engineering Corporation, China Construction Infrastructure Co., Ltd., Beijing 100013, China.

[3]Professor, Dept. of Disaster Mitigation for Structure, Tongji Univ., Shanghai 200092, China.

[4]Associate Professor, Dept. of Disaster Mitigation for Structure, Tongji Univ., Shanghai 200092, China.

Note. This manuscript was submitted on September 26, 2019; approved on October 16, 2020; published online on January 11, 2021. Discussion period open until June 11, 2021; separate discussions must be submitted for individual papers. This paper is part of the ***International Journal of Geomechanics***, © ASCE, ISSN 1532-3641.

where $d\varepsilon_v^p$ = the plastic volume strain increment; $d\varepsilon_d^p$ = the plastic deviatoric strain increment; M = the stress ratio in critical state; and η = stress ratio.

From Eq. (1), the M_c is equal to η in the critical state (M). Since M represents the upper limit of η, $d\varepsilon_v^p$ can only be positive and cannot be negative, which means it only represents shear shrinkage, not dilatancy.

To describe the dilatancy characteristics of OC soil, the MCC model could be extended; therefore, it could describe the particular behavior of OC clay. One of the most representative results of this is the UH model (Yao et al. 2008a, b, 2009, 2012; Yau and Kong 2012; Yau and Wang 2014), the UH model for OC clay has an added a unified hardening parameter under the MCC model framework, this means the model can describe some of the characteristics of OC clay, such as shear contraction, shear dilatancy, and strain hardening and softening when the overconsolidation degree equals zero, it will return to the MCC model naturally.

The model, which uses the Hvorslev line, is based on parabola to correct the potential strength parameters, and the parameters adopted in the UH model are identical to the MCC model. It is the most simple and practical constitutive model to describe the stress–strain relationship for OC clay. Similarly, Hashiguchi's subloading surface model (Hashiguchi 1989), and Nakai's (t_{ij}) model (Nakai 1989), are independently developed models within the framework of the MCC model. The subloading surface model assumes that there should be a subloading surface, which is geometrically similar to the normal yield surface in the stress space.

Since the point of current stress is always located on the subloading surface, the evolution of the geometric similarity ratio relationship between the subloading surface and normal yield surface can be described. Based on this, the constitutive equations that describe OC clay by analytical deduction can be obtained.

A generalization method proposed by Nakai (1989), based on the spatial mobilized plane (SMP) criterion, a yield surface equation expressed by the ordinary stress was introduced into T space by constructing a transformation tensor for the t_{ij} model, which can be adopted to describe the three-dimensional (3D) stress–strain relationship.

Another typical model is the boundary model proposed by Dafalias (1986). This model constructs a closed boundary that uses two ellipses and a hyperbola and deduces a plastic modulus formula for the boundary surface. The current plastic modulus can be obtained through the interpolating function in which the independent variable is the distance ratio of the current stress point to image point. The interpolation function is a total quantity given function, and it can describe the undrained strength of heavy OC clay more reasonably. However, there are too many parameters in this model, and some of them can not be determined experimentally. For example, there are 14 parameters in the boundary surface model proposed by Dafalias (1986). Conventional tests can determine the obtained parameters, such as the modulus of elastic volume compression (K), the corresponding slopes λ and κ of the normal consolidation line (NCL) and swelling line, Poisson's ratio (ν) for the NCLs and swelling line, and the η parameters (N_c) and (N_e) for the conventional triaxial compression and extension paths. Since the boundary surface in this model is a curve formed by splicing two elliptical curves with a hyperbolic curve in the middle, five parameters will be affected by the shape of the boundary surface, such as R_c, R_e, A_c, A_e, and T. R_c represents the proportional coefficient of the long and short axis of the large elliptic yield surface at the right end in the I-J space under the triaxial compression path, which is a stress-specific strength parameter. Geometrically, it is used to adjust the shape of the yield surface. Physically, it is a single-value function of the internal friction angle of triaxial compression, which is determined by the angle of internal friction. R_e corresponds to the strength parameter under the triaxial elongation path. Where A_c represents the distance coefficient between the vertex of the hyperbola segment and its asymptotic center point in the I-J space under the triaxial compression path. The slope of the projection of the Hvorslev surface in the I-J space can be determined by A_c. When $A_c = 0$, the projection of the Hvorslev surface in the I-J space is a diagonal segment that coincides with the CSL; when $A_c = \infty$, the projection of the Hvorslev surface in the I-J space is a horizontal segment; when the A_c value is between the previous values, the projection of the Hvorslev surface in the I-J space is an ordinary hyperbola. A_e represents the distance coefficient between the vertex and the center of the asymptote of the hyperbola that corresponds to the triaxial elongation path. The parameter T represents the proportional coefficient of tensile strength and pure compression hardening stress (I_0), which is used to determine the left end of the small ellipse at the left end of the yield surface and the left end of the I-axis. In addition, four parameters affected by the degree of overconsolidation, C, s, h_c, and h_e, are used to determine the influence law of different degrees of overconsolidation on deformation and strength. C is the parameter related to the projection center of the boundary surface. Its physical significance can be expressed as the proportional coefficient between the kinetic hardening stress (I_c) and the isotropic hardening stress (I_0) in the yield surface. s is the parameter used to determine the radius of the elastic domain. h_c and h_e, respectively represent the parameters of the influence factors for the shape hardening process of the boundary surface under the compression and extension paths. Between the previous parameters, the final four parameters all need to be calibrated to the experimental results to obtain reasonable parameter data. For the description of the dilatancy volume for clay Li and Li (2009) and Li and Dafalias (2004, 2012), introduced the state parameters to the dilatancy equation, which meant that the established constitutive model could reflect the shear contraction and dilatancy differences brought by the initial state differences. Gao et al. (2017) constructed a variable stress ratio with the boundary model as the frame and the similarity ratio as the independent variable and introduced this into the stress dilatancy equation, which could reflect the dilatancy volume differences for different degrees of overconsolidation. However, the parameters for the correction boundary shape changed with the overconsolidation, and it remains uncertain whether the shape of the yield surface relates to the degree of overconsolidation.

Based on disturbed state concept (DSC), a typical hierarchical single-surface (HISS) model was developed by Desai et al. (1986) and Desai and Toth (1996). The reactions of different complex degrees are described with δ_0, δ_1, δ_2, and δ_{vp}, such as associated isotropic hardening, unrelated isotropic hardening, anisotropic hardening, and viscoplasticity. The HISS model better reflects the effect of shear deformation and volumetric deformation on the hardening and yield of geotechnical materials. The concept of disturbance state is to set up a relative complete state first, then set up a complete disturbance state, then any load path or environmental impact could cause a semidisturbance state between the two. For natural OC soil, the following two assumptions should be satisfied: (1) soil samples with a relatively complete state and completely disturbed state need to be composed of the same microscopic components and mineral proportions: and (2) maintain the initial integrity of overconsolidation before loading was carried out. However, during the construction of the disturbance function, the main method was deductive using soil mechanics principles or mathematical means. There are more subjective assumptions, and lower theoretical basis and experimental support; therefore, there are some difficulties in the determination of the disturbance function and the corresponding parameters.

Because the UH model does not have perfect simulation for the dilatancy of OC soil, two improvements are made based on the

overconsolidated UH model. The first uses an initial state parameter to reflect the larger volume compression characteristics of the unconsolidated soil, which introduces the state parameter (χ) to the yield surface equation, to reflect the increased volume compaction characteristics of UC clay.

The second uses the nonassociative flow rule. The M_c of the plastic potential surface can be expressed as the power function of the initial consolidation stress ratio (R), it can be employed to reflect the change law of the M_c that corresponds to various overconsolidation degrees. The shrinkage volume reduces with the increase of the overconsolidation degree, meanwhile, the shear dilatancy volume increases.

However, the modified model extends the description range for clay from overconsolidation to underconsolidation; therefore, it produces more accurate results for the description of the dilatancy characteristics of OC clay.

Brief Review of UH Model

Fig. 1 shows the state of stress and void ratio of OC soil in e-ln$p$ space. Point A′ in this figure is unloaded from point B′. For point A′, the corresponding preconsolidation pressure is point B′. Therefore, according to the definition of the degree of superconsolidation, the following is obtained: $R = p_x/\bar{p}_x$. Corresponding to R as shown in Fig. 2, the previously defined R is the geometric similarity ratio between the current yield surface and the reference yield surface. The basic principle of the UH model is to take R of the degree of overconsolidation as an initial state parameter. The influence of this initial state parameter (R) on the OC soil is based on deformation and strength. The basic idea of modeling was as follows. First, the relationship between R and the strength of the Hvorslev line was established through different degrees of overconsolidation. Then, the relationship between the strength of the Hvorslev line and the potential strength stress ratio (M_f) was established. M_f was used to construct the uniform hardening parameters. The uniform hardening parameters were used to reflect the laws of volume shrinkage, dilatation, stress hardening and strain softening. Therefore, a parameter R, which reflects the initial R, was introduced to reflect the laws of OC soil, such as contraction before dilatation, strain hardening, and strain softening. The interrelationship between R, M_f, and UH parameter H is shown in Fig. 3. Since OC clays with different overconsolidation degrees might have different potential strengths of η, the value of M_f is related to R. Besides, the UH parameter H is related to M_f. Therefore, H was affected by M_f. Meanwhile, the evolution of UH parameter H (related to ε_v^p) determined the relative locations between the current yield surface and the reference yield surface, which conversely influenced the evolution law of R.

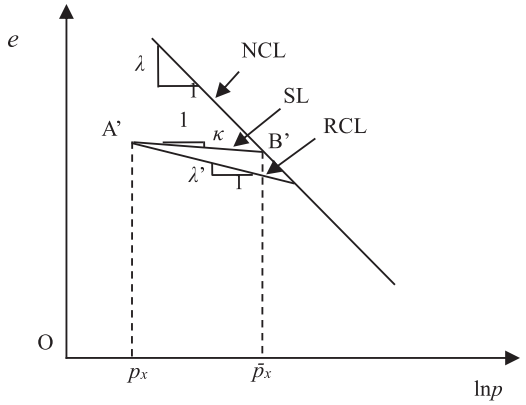

Fig. 1. Schematic diagram of reloading curve of OC clay.

Therefore, a circulatory relationship between R, M_f, and UH parameter H was established, as shown in Fig. 3. This interdependent relationship remained valid when the OC clay degenerated into the NC clay.

Fundamental Equation of the Modified UH Model

Refer to the Yield Surface and the Current Yield Surface Equation

The reference yield surface equation adopted can be expressed as

$$\bar{f} = \ln\frac{\bar{p}}{\bar{p}_0} + \ln\left(1 + \frac{\eta^2}{M^2 - \chi\eta^2}\right) - \frac{\varepsilon_v^p}{c_p} = 0 \tag{2}$$

The current yield surface equation can be expressed as

$$f = \ln\frac{p}{p_0} + \ln\left(1 + \frac{\eta^2}{M^2 - \chi\eta^2}\right) - \frac{1}{c_p}\int\frac{M_f^4 - \eta^4}{M_c^4 - \eta^4}d\varepsilon_v^p = 0 \tag{3}$$

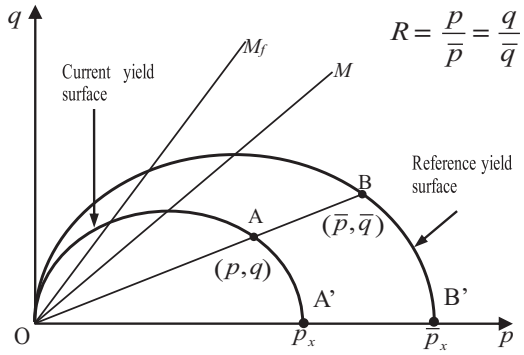

Fig. 2. Current yield surface and reference yield surface of UH model.

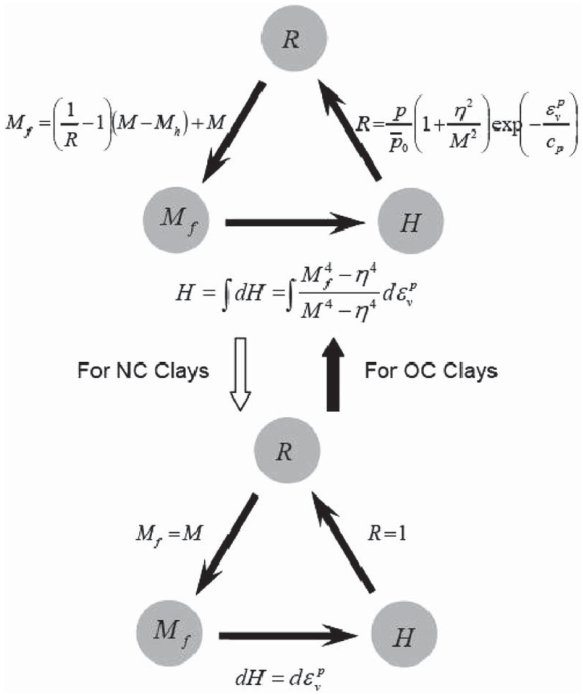

Fig. 3. Relationship between R, M_f, and UH parameter H.

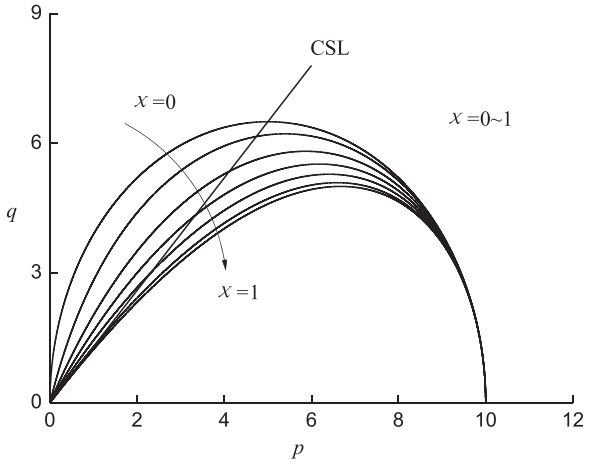

Fig. 4. The yield surface that corresponds to different values of χ.

The equation of plastic potential surface is

$$g = \ln\frac{p}{p_0} + \ln\left(1 + \frac{\eta^2}{M_c^2}\right) - \frac{1}{c_p}\int\frac{M_f^4 - \eta^4}{M_c^4 - \eta^4}d\varepsilon_v^p = 0 \tag{4}$$

where $\bar{p}$ = the mean stress at a point on the reference yield surface; $\bar{p}_0$ = the reference initial average stress that corresponds to p_0; χ = the initial state parameter; η = the stress ratio that is equal to q/p; ε_v^p = the plastic volume strain; c_p = a constant expression that consists of parameters; $c_p = (\lambda - \kappa)/(1 + e_0)$; M = critical state stress ratio; p and p_0 = the average stress on the current yield surface and the initial average stress; M_c = the variable stress ratio that represents the stress ratio that corresponds to the transition time of bulk strain from shear contraction to dilatation, or the stress ratio that corresponds to the transition time from positive pore pressure to negative pore pressure; and M_f = the potential strength stress ratio and represents the concept of the strength potential of the OC soil.

Fig. 4 shows the corresponding yield surface shape, from ellipse to water drop shape, when χ is 0, 0.1, 0.3, 0.5, 0.7, 0.9, and 1, respectively. Here, p is effective mean stress and q is the generalized deviatoric stress. They can be expressed by using principal stresses

$$p = \frac{\sigma_1 + \sigma_2 + \sigma_3}{3} \tag{5}$$

$$q = \frac{1}{\sqrt{2}}\sqrt{(\sigma_1 - \sigma_2)^2 + (\sigma_2 - \sigma_3)^2 + (\sigma_3 - \sigma_1)^2} \tag{6}$$

As shown in Fig. 5, the three skew lines that are parallel to each other represent the NCL, CSL, and the densest consolidated line (DCL), respectively. It was assumed that the DCL was the upper limit of the density, for example, the lower limit of the corresponding void ratio. Loading tests with a constant P were carried out from the four different initial points A, B, D, and G, respectively. Because point A was located on the NCL, the whole shearing process remained in a constant shrinkage state. Along the AC path directly to the CSL C, the corresponding volume strain value was $c_p \ln 2$. When the initial point was located in the area that was below the NCL line but above the DCL line, such as the point D, which shrank to point E first and then began to dilate until point F. When the initial point was B, due to the corresponding state during maximum dense status under the current mean stress, dilatancy processes during the whole process of shear loading and reached from point B to point C. When the initial point was located in the area above the NCL line, such as point G, the corresponding

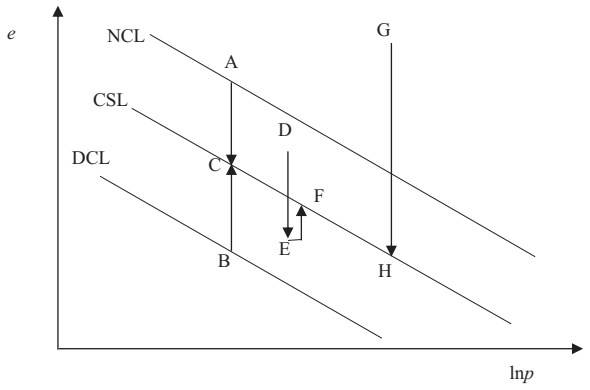

Fig. 5. The variation law of pore ratio under the load of equal p stress path that corresponds to different initial states.

state was UC soil. At this point, it sheared directly along the GH path loading to H with the whole shear contraction state.

The NCL equation can be expressed as follows:

$$e = N - \lambda \ln p \tag{7}$$

The CSL equation can be expressed as follows:

$$e = \Gamma - \lambda \ln p \tag{8}$$

The DCL equation can be expressed as follows:

$$e = D - \lambda \ln p \tag{9}$$

where e = the void ratio; λ = the slope of NCL in e-ln$p$ space; N = the intercept of NCL in e-ln$p$ space; Γ = the intercept of CSL in e-ln$p$ space; and D = the intercept of DCL in e-ln$p$ space.

For the UC clay, the shear contraction degree during the shear contraction process can be expressed by the parameter χ. It was assumed that the process from G to H can be expressed by a volume change equation as follows:

$$\varepsilon_v^p = c_p\left[\ln\frac{p}{p_0} + \ln\left(1 + \frac{\eta^2}{M^2 - \chi\eta^2}\right)\right] \tag{10}$$

Eq. (10) is based on the relationship between the p process of the unconsolidated soil and point H, as shown in Fig. 2. When Eq. (2) is loaded along the constant mean stress path, $dp = 0$; when it is loaded into the critical state, $p = p_0$, $\eta = M$ can be substituted into the Eq. (8).

Considering p remains a constant value during the loading process, the simplified equation is as follows:

$$\varepsilon_v^p = c_p \ln\left(1 + \frac{1}{1 - \chi}\right) \tag{11}$$

If the plastic volume change equals volume strain, then

$$\varepsilon_v^p = \varepsilon_v = \frac{\Delta e}{1 + e_0} = \frac{e_0 - \Gamma + \lambda \ln p_0}{1 + e_0} \tag{12}$$

where Δe = the change value of void ratio. Combining Eqs. (11) and (12), expression of parameter χ can be obtained

$$\chi = 1 - \frac{1}{\exp\left(\frac{e_0 - \Gamma + \lambda \ln p_0}{\lambda - \kappa}\right) - 1} \tag{13}$$

where κ = the slope of swelling line that corresponds to the NCL in e-ln$p$ space. When e_0 is on the NCL line, the following

is obtained:

$$\chi = 1 - \frac{1}{\exp(\ln 2) - 1} = 0 \tag{14}$$

When Eq. (10) is true, the shape of yield surface is an ellipse.

When e_0 is above NCL line, the following expression can be obtained:

$$\Delta e > (\lambda - \kappa)\ln 2 \tag{15}$$

Combining Eqs. (14) and (15), the following expression that corresponds to an initial underconsolidated state can be obtained:

$$0 < \chi = 1 - \frac{1}{\exp\left(\frac{\Delta e}{\lambda - \kappa}\right) - 1} < 1 \tag{16}$$

Therefore, the values of the parameter χ can be determined according to the ratio of the initial void ratio to the void ratio under the same mean stress on the NCL

$$\chi = \begin{cases} 1 - \dfrac{1}{\exp\left(\dfrac{e_0 - \Gamma + \lambda \ln p_0}{\lambda - \kappa}\right) - 1} & e_0 > e_n \\ 0 & e_0 \le e_n \end{cases} \tag{17}$$

Dilatancy Equation

From Eq. (4), it is known that the dilatancy equation can be expressed as follows:

$$\frac{d\varepsilon_v^p}{d\varepsilon_d^p} = \frac{M_c^2 - \eta^2}{2\eta} \tag{18}$$

Therefore, the expression of M_c can be determined by R_0, which can be expressed by the following equation:

$$M_c = MR^{R_0} \tag{19}$$

where R_0 = the initial value of R.

M_f can be expressed as follows:

$$M_f = 6\left(\sqrt{k_p(1 + k_p)} - k_p\right) \tag{20}$$

$$k_p = \frac{M^2}{12(3 - M)R} \tag{21}$$

Eqs. (20) and (21) can be used to calculate M_f. The Hvorslev line is a common index to measure the undrained shear strength of OC clay. Traditionally, the Hvorslev line is used as the envelope of the undrained shear strength of clay and the boundary of the physical state of the superconsolidated clay in the p-q space. For the heavy OC soil, the traditional method is to use the zero tensile stress line as the boundary line. The above double broken lines were used as the reference strength envelope to calculate M_f. However, the adoption of a zero tensile stress line will result in the inherent defect that η is >3, and the intersection point between the two broken lines will cause singularity. The UH model (Yao et al. 2012) uses parabola to replace the Hvorslev strength envelope of the previous double fold line, which solves the two basic problems inherent in the previous double fold line. Eqs. (20) and (21) are used to calculate M_f by using parabola as the strength envelope of the Hvorslev line. It effectively described the phenomenon that the η of heavily OC soil increased with the increase of the degree of overconsolidation. The law of dilatancy increased and the rule that the M_c decreased with the increase of the degree of overconsolidation proposed in this study could be reflected.

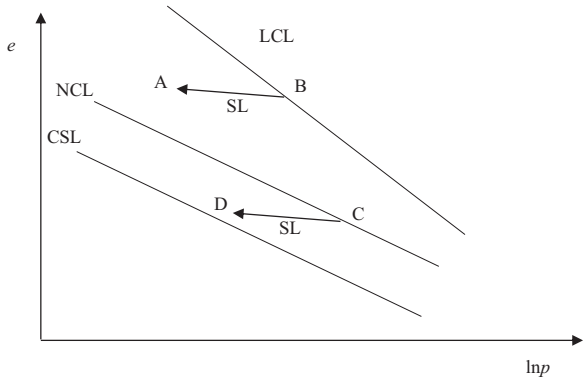

Fig. 6. The overconsolidation R determined by the swelling line at different initial states.

In Eq. (20), k_p is a temporary variable. Then, R can be expressed as follows:

$$R = \frac{p\left[1 + \dfrac{(\eta/M)^2}{1 - \chi(\eta/M)^2}\right]}{\bar{p}_0 \exp(\varepsilon_v^p / c_p)} \tag{22}$$

For unconsolidated soils, the initial void ratio is always greater than the void ratio at the same mean stress due to the failure of the normal consolidation process of NCL.

As shown in Fig. 6, for the OC clay, when the stress state point goes along the NCL line compressed to point C and then is unloaded to point D, the current overconsolidation ratio (OCR) = $1/R = p_C/p_D$, $R = p_D/p_C$. But, for the UC clay, when the initial state is on point A, the preconsolidation pressure can not be found on the NCL, by considering the e-ln$p$ space, a loosest consolidation line exists (LCL) for the initial state of e_A, p_A, the preconsolidation pressure p_B can always be found on the LCL through the swelling line. Due to the failure of consolidation, the parameter R can be expressed as $R = p_A/p_B$. The LCL can be expressed as

$$e = \mathrm{T} - \alpha \ln p \tag{23}$$

where T = the slope of the LCL in e-ln p space. For the definition of M_c, it can be redefined as

$$M_c = \begin{cases} M & e_0 > e_n \\ MR^m & e_0 \le e_n \end{cases} \tag{24}$$

The relationship between parameter m and M_c is shown in Fig. 7.

Model Constitutive Equation

The incremental elastoplastic constitutive relation was used in this model, the total strain increment can be divided into two parts: elastic strain increment and plastic strain increment, the relationship between these two parts can be expressed as follows:

$$d\varepsilon_{ij} = d\varepsilon_{ij}^e + d\varepsilon_{ij}^p \tag{25}$$

The elastic strain increment can be obtained by the generalized Hooke's law

$$d\varepsilon_{ij}^e = \frac{1 + \nu}{E} d\sigma_{ij} - \frac{\nu}{E} d\sigma_{mm}\delta_{ij} \tag{26}$$

where E = the modulus of elasticity; and ν = Poisson's ratio.

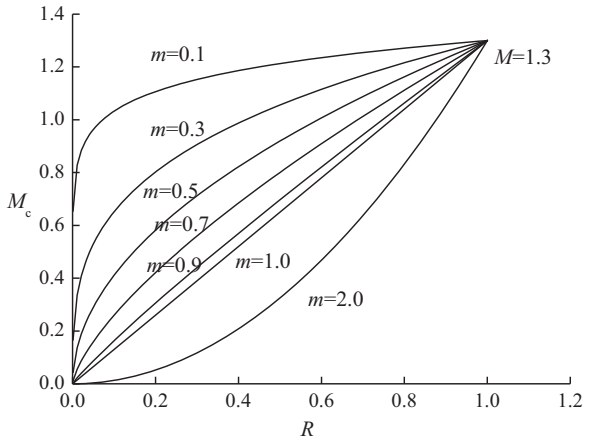

Fig. 7. The change rule for M_c with R in different values of parameter m.

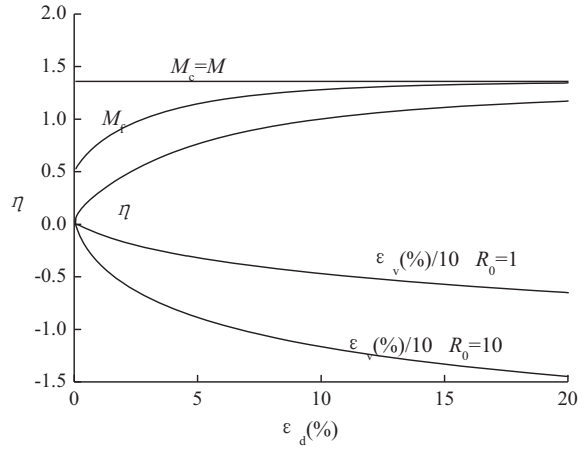

Fig. 9. Evolution rule of strength parameter with deviatoric strain at $R_0 = 10$.

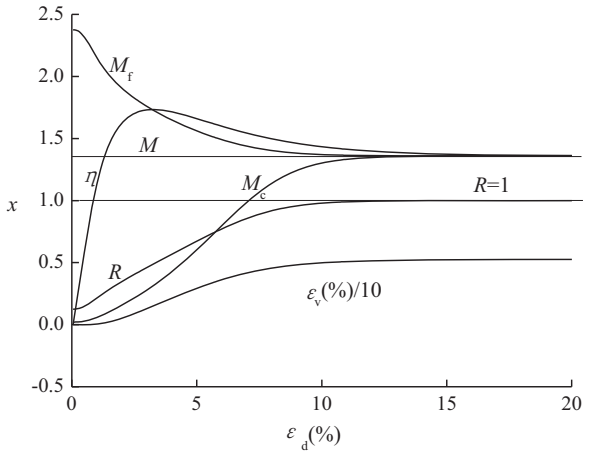

Fig. 8. Evolution law of strength parameter with deviatoric strain at OCR = 8.

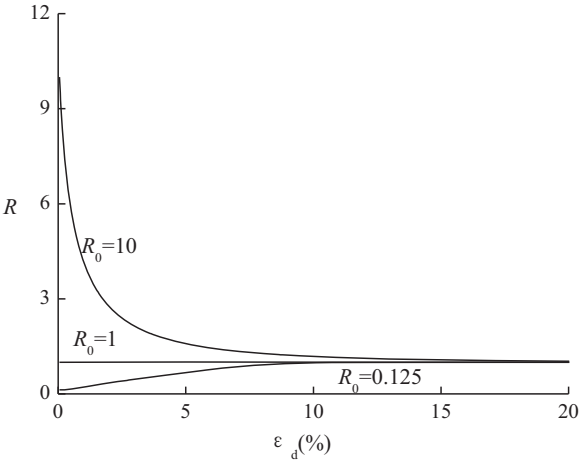

Fig. 10. Evolution rule of R with deviatoric strain at different initial values of R_0.

E can be expressed as

$$E = \frac{3(1-2\nu)(1+e_0)p}{\kappa} \tag{27}$$

The increment plastic strain can be obtained by the consistency law

$$d\varepsilon_{ij}^{p} = \Lambda \frac{\partial g}{\partial \sigma_{ij}} \tag{28}$$

where $\Lambda =$ the plastic factor. It can be deduced by the consistent condition of yield surface equation.

Fig. 8 shows the stress–strain relationship of a typical OC soil and the evolution law of strength parameters. When the initial state is OCR = 8 and under the conventional triaxial compression condition, with the increase of deviatoric strain, the stress ratio shows the phenomenon of strain hardening and strain softening. At the same time, the shrinkage occurred first and then dilatancy was observed. The parameter R increased gradually from the initial value from 0.125 to 1, when the deviatoric strain reached 20%, which showed that the degree of OC decreased gradually with the loading process. The M_c increased gradually from the initial value that was slightly >1, and when it intersected η, the conversion point of shear shrinkage and dilatancy appeared. When η was $>M_c$ it will always be in the dilatancy state, the potential strength (M_f) gradually decays with loading. After the intersection with η, which was greater than the value of M_f, this will result in the hardening parameter increment $dH < 0$, the plastic modulus in a state of decay, which caused η to decreases gradually and the formation of strain softening.

When the initial value $R_0 = 10$, η began to increase, approaching M, M_f increased gradually from the initial value, which was slightly >0.5, meanwhile, M_c was always equal to M. For the hardening parameter, due to $M_f < M_c$, this resulted in the coefficient of hardening parameter $\Omega = (M_f^4 - \eta^4)/(M_c^4 - \eta^4) < 1$, which caused the volume change, where the plastic volume strain is greater than that for OCR = 1. The volume change of $R_0 = 10$, as shown in Fig. 9 is significantly larger than that for $R_0 = 1$.

Evolution curves that correspond to three initial values of R during loading are shown in Fig. 10. The value of deviatoric strain gradually reached 20%, and the different initial values of R approached 1 at this point. For example, when the values of R_0 were 10, 1, and 0.125, respectively, the values of R tended to approach 1 during the loading process.

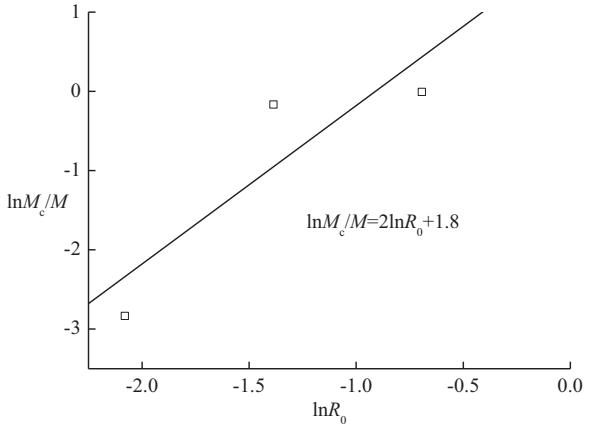

Fig. 11. Calibration of the value of M_c according to R_0 which is the initial value of R.

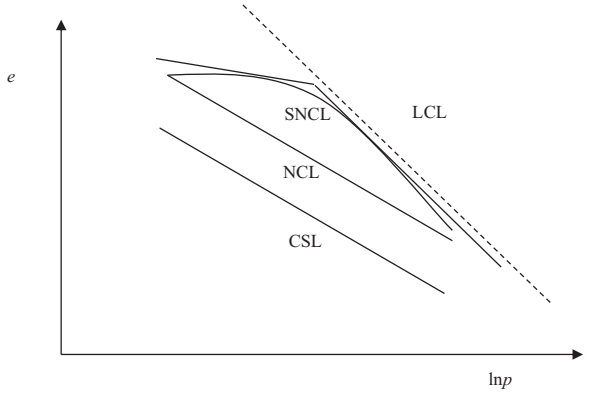

Fig. 12. Calibration of LCL for clay under isotropic compression loading conditions.

Parameter Calibration

Calibration of M_c

From Eq. (22), M_c is always the function of parameter R. At the transition point from volume shrinkage to expansion, the value of R is different from the initial value R_0. The value of R that corresponds to transition changes from R_0 to one during the loading process, it was assumed that R was relevant to the initial value of R_0 at the point of phase transformation. The relationship can be expressed as follows:

$$R^m = hR_0^m \tag{29}$$

The parameters m and h can be obtained by calibrating the test data. Therefore, the value of h is >1.

Combining Eq. (23) with Eq. (28), the following equation can be obtained:

$$\ln\frac{M_c}{M} = m\ln R_0 + \ln h \tag{30}$$

The discrete point shown in Fig. 11 is η at the transition point that is obtained from triaxial compression test carried out on Nakai on Fujinomori clay. For the different initial overconsolidation degree, OCR was selected as 2, 4, 8, the linearization relationship between η and R_0 with logarithmic transformation was established. The straight line fitted by the graph shows that the value of $m = 2$.

Calibration of Intercept and Slope for the LCL

From Eq. (19), there is an LCL in the e-ln p space, because the sample during the consolidation process always shows a certain degree of consolidation, it is difficult to reach the ideal loosest state; therefore, an asymptote in the isotropic compression line family can be used as the LCL.

There will always be a certain degree of cementation for natural clay during the deposition process, which means that the clay possesses a natural structure. For the isotropic compression line, it normally presents two typical curve modes that are first straight, then declined rapidly. The NCL shown in Fig. 10 is the normal compression line for consolidated remolded clay, the CSL is shown, and structure normal compression line (SNCL) is the compression line with a certain structure. In general, due to the characteristics of the platform for the SNCL, the SNCL can be presented by two linear asymptotes. Therefore, all the lines with certain structural characteristic can be presented by the previous two linear asymptotes. The LCL can be presented by the linear asymptote of the second phase that is indicated by the dashed line shown in Fig. 10.

Table 1. Parameters of material

Parameter	Boston blue clay	Kaolin clay	Black kaolinite clay	Fujinomori clay
M	1.15	1.04	0.82	1.36
λ	0.09	0.34	0.085	0.09
κ	0.02	0.058	0.024	0.02
ν	0.3	0.3	0.3	0.3
m	0.2	0.2	0.2	2
T	1.5	1.5	1.5	1.5
α	0.11	0.11	0.11	0.11
e_0	1.01	0.95	1.29	0.83
p_0(kPa)	300	200	161	98

Calibration Rest of Parameters

As shown Fig. 12 there are lines to obtain some of the parameters. For the rest of the parameters, because it was based on the UH model for OC clay, the rest of the parameters were identical to those in the MCC model. M, ν, the slope of compression line (λ), and the slope of swelling (κ), were determined by triaxial compression and oedometer tests.

Model Validation

To verify the applicability and rationality of the modified model, a series test results from clay were used to verify the predictive performance of the model. The values of the parameters for four types of clays are displayed in Table 1. The discrete points shown in Figs. 13 and 14 are the test results for Boston blue clay under undrained triaxial compression conditions by Pestana and Whittle (1999). The overconsolidation degree was 1, 2, 4, and 8, respectively. The preconsolidation pressure was used as the normalized mean stress. Fig. 11 shows that for the consolidated clay, the predicted shear modulus agreed with the test results, but the predicted ultimate strength values overestimated the actual results. Due to some OC degree, the value of χ equals 0.15 when OCR = 1. When OCR = 4 and 8, the predicted shear modulus was slightly lower than the actual results, the ultimate stress ratio strength value predicted was consistent with that of the test. From the effective stress path shown in Fig. 14, the volume shrinkage for the

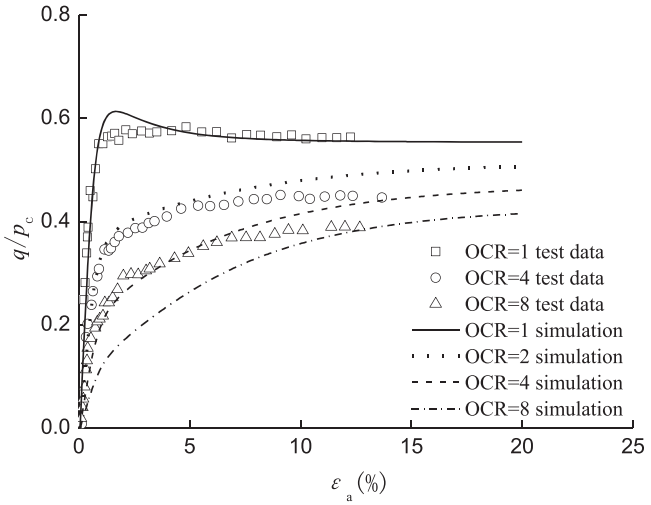

Fig. 13. Comparison of predicted and test results between η and axial strain for Boston blue clay.

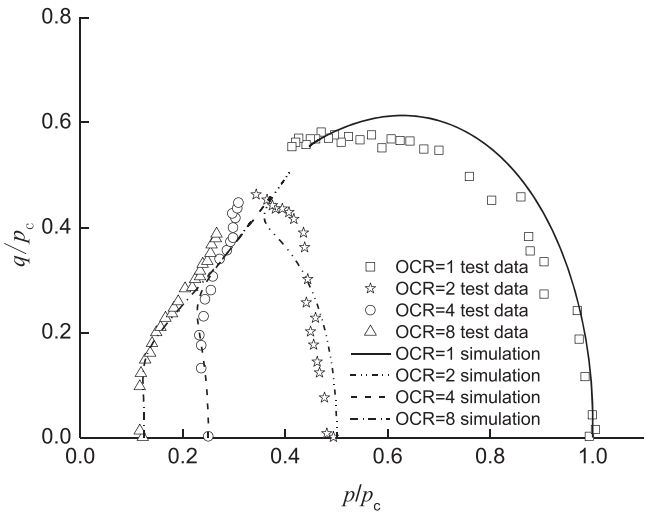

Fig. 14. Comparison of predicted and test results for effective stress path of Boston blue clay.

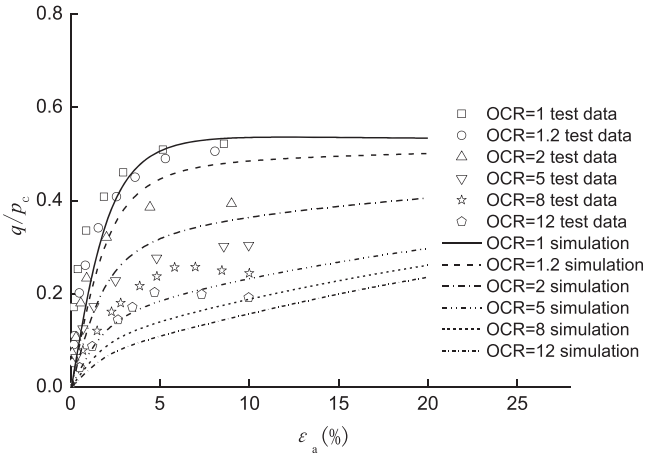

Fig. 15. Comparison of predicted and test results between η and axial strain for Kaolin clay.

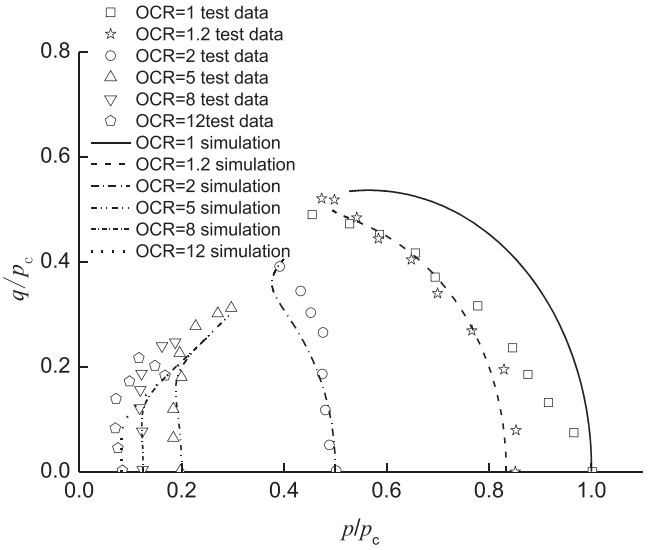

Fig. 16. Comparison of predicted and test results for effective stress paths for Kaolin clay.

measured value for NC clay was larger and softer than that of the predicted value. Comparison was shown when the OC degree was 4, 8, the shear dilatancy was overestimated, meanwhile, the stress strength ratio was the same. For the shear contraction, which appeared during the final stage when the OC degree = 2, which is different from the predicted result for dilatancy, it was considered that the structural behavior of clay affected the dilatancy by preliminary analysis. As shown in Fig. 13, the test data for OCR = 2 was neglected. The experiment with OCR = 2 had some technical difficulties and the stress–strain response was not considered reliable. Based on the clay sample with a smaller OCR, there were usually some structural effects in saturated clay, especially in light and OC clay. The influence of the structure on deformation resulted in a larger volumetric strain and a higher strength η than that of remolded clay under shear loading. This will interfere with the law of the influence of the degree of overconsolidation on the volume–strain to intensity–stress ratio. Therefore, through the analysis, it was concluded that there was a natural structural influence problem.

The discrete points shown in Figs. 15 and 16 are the results of the triaxial undrained shear test for Kaolin clay carried out by Stipho (1978), and the fine line was used to predict the results of the modified model. Different initial consolidation states for OC degree were 1, 1.2, 2, 5, 8, and 12. As shown in Fig. 15, in the two cases of OCR = 1 and 1.2, the predicted values overestimated the experimental results. Due to some OC degree, the value of χ = 0.1 when OCR = 1. Compared with the actual loading path, the experimental results show greater shrinkage characteristics and were softer than the predicted value. When OCR = 2, 5, 8, and 12, the stress ratio curves, and stress paths were consistent with the experimental results. This shows that under the lower OCR, the cementation characteristics of soil samples always had a negligible effect on dilatancy. The direct performance was the greater volume compression characteristics and greater positive pore pressure.

The discrete points shown in Figs. 17 and 18 are the test results of conventional drained triaxial compression on the Black kaolinite clay by Zervoyanis (1982), the curve is the predicted result of the model. Compared with the results with an OC degree of 1, 2, 4, and 8, this shows that during the NC clay shear process, the volume shrinkage was larger than the predicted value, meanwhile, the shear modulus was smaller than the predicted value. When OCR = 2, 4,

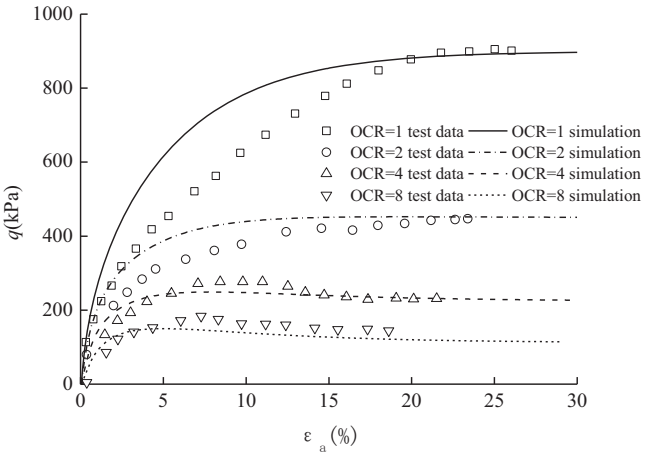

Fig. 17. Comparison of predicted and test results between η and axial strain for Black kaolinite clay.

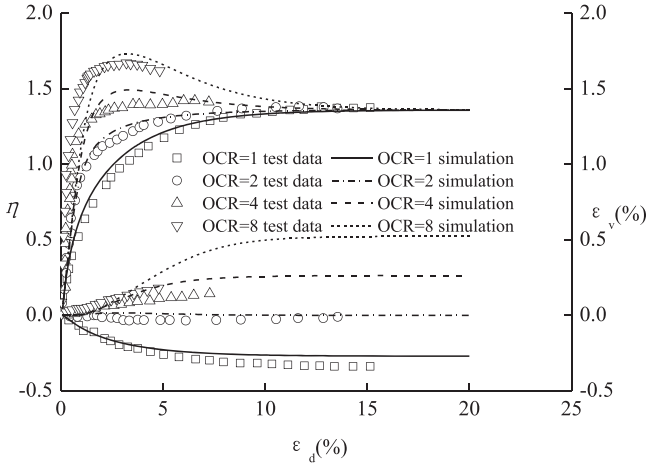

Fig. 19. Comparison of predicted and test results for triaxial compression for Fujinomori clay.

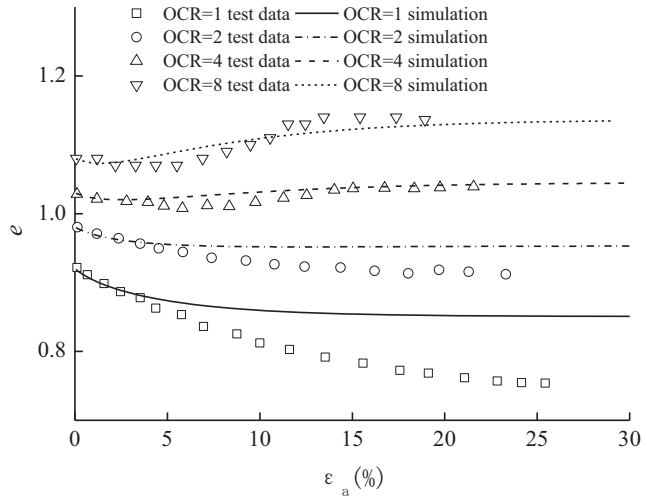

Fig. 18. Comparison of predicted and test results for void ratio change process for Black kaolinite clay.

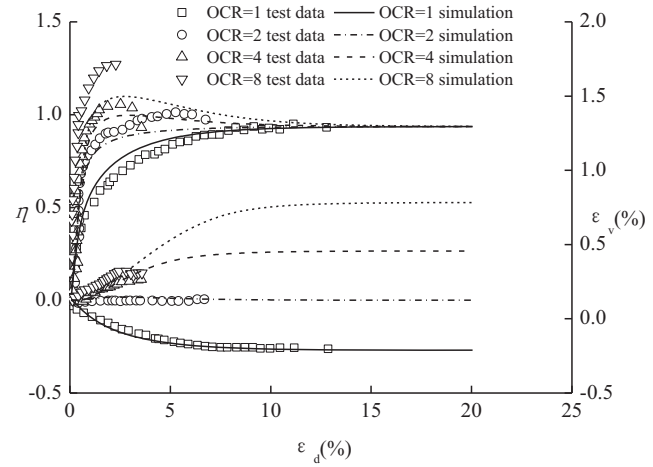

Fig. 20. Comparison of predicted and test results for triaxial extension for Fujinomori clay.

and 8, both the deviatoric stress and the void ratio predicted values were in good agreement with the experimental results. The material softening phenomenon shown during the loading process for deviatoric stress could be reflected by the modified model. In addition, the void ratio decreased first and then increased, which shows that the modified model could reflect the deformation characteristics of dilatancy after shrinkage.

The discrete points shown in Figs. 19 and 20 are the results of triaxial compression and triaxial extension tests under the drained P path on Fujinomori clay carried out by Nakai and Hinokio (2004). The mean stress for OCR = 8 was controlled at 98 kPa, and for the remaining OCR samples, the mean stress was controlled at 196 kPa. By comparing triaxial compression, predictive stress ratio was consistent with the measured values, the coordinate value of volume change result could be presented by the coordinate on the right. This shows that with the increase of OCR, soil shear shrinkage decreased, the dilatancy amount increased gradually, and with the increase of OCR, η decreased at the occurrence of the corresponding expansion. As shown in Fig. 19, except for the stress ratio strength value OCR = 8 was smaller than that of the measured value, the other stresses predicted agreed with the measured values. The characteristics of dilatancy after shrinkage and M_c that reduced with the increase of OCR could be reflected by the proposed model. As shown in Figs. 19 and 20, under the same OCR, the predicted value of η that corresponds to the triaxial compression was greater than that of triaxial extension for the same axial strain. This means that the transformed stress method could effectively be adopted to influence the stress of Lode's angle for critical state strength characteristics.

One of the phenomena shown in Figs. 19 and 20 is strain softening. However, during the process of loading, strain localization occurs, and strain localization leads to strain softening of macroscopic phenomena. The experimental results shown in Figs. 19 and 20 were aimed at the soil unit to strictly eliminate the formation of the strain localization, which meant that only the mechanical properties of the unit, not the strain softening caused by the strain localization, was induced by this structural damage.

Due to the influence of many factors during the experimental loading process, for example, the clay sample could not form an ideal uniform continuous unit during the preparation process, and some local shear bands were formed during the shear loading process, which resulted in the strain localization problem. In addition, there was a structural influence in the clay sample, and the presence

of clay structure increased the probability of strain localization. The strain localization reduced the final η strength value, and the predicted value was slightly higher than the experimental η strength value. Although the modified UH model proposed in this study could simply and reasonably consider the nature of the influence of the degree of overconsolidation on the law of dilatation deformation, it means that the law of the influence of the degree of overconsolidation on the strength of the disguised η was reasonably reflected. The modified UH model proposed in this study was used to describe the effect of the stress ratio degree of overconsolidation on the deformation and η strength in a detailed and rigorous manner. However, the modified model proposed in this study has some limitations, for example, natural clay often has a certain degree of structural and creep properties. However, the influence of the proposed modified UH model on the stress–strain relationship between the structure and creep properties of natural clay could not be reasonably considered. In addition, this is the direction of future research to improve the model of the modified model proposed in this study.

Conclusion

Since the UH model could not reflect the decrease characteristics of phase transformation stress decrease with increasing OCR or the larger volume compression characteristics for UC clay, the modified model was proposed based on the UH model. The nonassociated flow rule was adopted, because it could modify the yield surface equation using the state parameter that reflected the underconsolidation state, and it reflected the M_c of OC soil's plastic potential surface, a power function was used to modify the strength parameter, which could satisfy the change rule for the conversion point η of shear shrinkage to dilatancy. It could be adopted to calculate the amount of shear shrinkage and dilatancy compression more easily. According to the comparison of prediction and test results, the following conclusions were obtained:

1. The modified model was applied to extend the applicability of the OC soil UH model, which extended the state of NC soil and OC soil to the state of UC soil. The state parameters introduced in the model could reflect the larger volume compression characteristics of the UC soil more simply and reasonably.
2. Using a power function of R to modify the M_c, which introduced this M_c into the plastic potential surface equation and the hardening parameter, which could be effectively adopted to simulate the η transition point from shear shrinkage to dilatancy. It was more reasonable to estimate both the process and the result of the volume strain.
3. Transformation stress could be used as a simple and direct way to extend the modified model to a general model, and it could be effectively adopted to simulate the stress–strain relationship for the soil element under the 3D stress loading path. By comparing a series of predicted and test results for clay, it confirmed that the model was simple and effective to simulate the general stress–strain relationship for the UC and OC soil.

Data Availability Statement

All data, models, and code generated or used during the study appear in the published article.

Acknowledgments

This study was supported by the National Natural Science Foundation of China for young scholars (Grant No. 11402260). The department of housing and urban-rural development of science and technology plan projects under Grant No. 20151602420730018, and the Foundation of China Academy of Building Research under Grant Nos. 20141602336230036, 20141602330730038, and 20171602330710007.

References

Asaoka, A. 2004. "Consolidation of clay and compaction of sand-an elastoplastic description." In *Proc., 12 Asian Regional Conf. on Soil Mechanics and Geotechnical Engineering*, 1157–1195. Singapore: World Scientific Publishing Company.

Banerjee, P. K., and N. B. Yousif. 1986. "A plasticity model for the mechanical behaviour of anisotropically consolidated clay." *Int. J. Numer. Anal. Methods Geomech.* 10 (5): 521–541. https://doi.org/10.1002/nag.1610100505.

Casagrande, A., and N. Carillo. 1944. "Shear failure of anisotropic materials." *Boston Soc. Civ. Eng. J.* 31 (2): 74–87.

Dafalias, Y. F. 1986. "Bounding surface plasticity I: Mathematical foundation and hypoplasticity." *J. Eng. Mech.* 112 (9): 966–987. https://doi.org/10.1061/(ASCE)0733-9399(1986)112:9(966).

Desai, C. S., S. Somasundaram, and G. Frantziskonis. 1986. "A hierarchical approach for constitutive modeling of geologic materials." *Int. J. Numer. Anal. Methods Geomech.* 10 (3): 225–257. https://doi.org/10.1002/nag.1610100302.

Desai, C. S., and J. Toth. 1996. "Disturbed state constitutive modeling based on stress-strain and nondestructive behavior." *Int. J. Solids Struct.* 33 (11): 1619–1650. https://doi.org/10.1016/0020-7683(95)00115-8.

Gao, Z. W., J. D. Zhao, and Z. Y. Yin. 2017. "Dilatancy relation for overconsolidated clay." *Int. J. Geomech.* 17 (5): 06016035. https://doi.org/10.1061/(ASCE)GM.1943-5622.0000793.

Hashiguchi, K. 1989. "Subloading surface model in unconventional plasticity." *Int. J. Solids Struct.* 25 (8): 917–945. https://doi.org/10.1016/0020-7683(89)90038-3.

Jovicic, V., and M. R. Coop. 1998. "The measurement of stiffness anisotropy in clays with bender elements tests in the triaxial apparatus." *Geotech. Test. J.* 21 (1): 3–10. https://doi.org/10.1520/GTJ10419J.

Li, X. S., and Y. F. Dafalias. 2004. "A constitutive framework for anisotropic sand including non-proportional loading." *Géotechnique* 54 (1): 41–55. https://doi.org/10.1680/geot.2004.54.1.41.

Li, X. S., and Y. F. Dafalias. 2012. "Anisotropic critical state theory: Role of fabric." *J. Eng. Mech.* 138 (3): 263–275. https://doi.org/10.1061/(ASCE)EM.1943-7889.0000324.

Li, X. S., and X. Li. 2009. "Micro-macro quantification of the internal structure of granular materials." *J. Eng. Mech.* 135 (7): 641–656. https://doi.org/10.1061/(ASCE)0733-9399(2009)135:7(641).

Ling, H., D. Yue, V. Kaliakin, and N. Themelis. 2002. "Anisotropic elastoplastic bounding surface model for cohesive soils." *J. Eng. Mech.* 128 (7), 748–758. https://doi.org/10.1061/(ASCE)0733-9399(2002)128:7(748).

Matsuoka, H., and K. Sakakibara. 1987. "A constitutive model for sands and clays evaluating principal stress rotation." *Soils Found.* 27 (4): 73–88. https://doi.org/10.3208/sandf1972.27.4_73.

Nakai, T. 1989. "An isotropic hardening elastoplastic model for sand considering the stress path dependency in three-dimensional stresses." *Soils Found.* 29 (1): 119–137. https://doi.org/10.3208/sandf1972.29.119.

Nakai, T., and M. Hinokio. 2004. "A simple elastoplastic model for normally and over-consolidated soils with unified material parameters." *Soils Found.* 44 (2): 53–70. https://doi.org/10.3208/sandf.44.2_53.

Oda, M., and J. Konishi. 1974. "Microscopic deformation mechanism of granular material in simple shear." *Soils Found.* 14 (4): 25–38. https://doi.org/10.3208/sandf1972.14.4_25.

Ohta, H., and A. Nishihara. 1985. "Anisotropy of undrained shear strength of clays under axi-symmetric loading conditions." *Soils Found.* 25 (2): 73–86. https://doi.org/10.3208/sandf1972.25.2_73.

Pestana, J. M., and A. J. Whittle. 1999. "Formulation of a unified constitutive model for clays and sands." *Int. J. Numer. Anal. Methods Geomech.* 23 (12): 1215–1243.https://doi.org/10.1002/(SICI)1096-9853(199910)23:12<1215::AID-NAG29>3.0.CO;2-F.

Reynolds, O. 1885. "On the dilatancy of media composed of rigid particles in contact. With experimental illustrations." *Philos. Mag. J. Sci.* 20 (127): 469–481. https://doi.org/10.1080/14786448508627791.

Roscoe, K. H., A. N. Schofield, and A. Thurairajah. 1963. "Yielding of clays in states wetter than critical." *Géotechnique* 13 (3): 211–240. https://doi.org/10.1680/geot.1963.13.3.211.

Rouainia, M., and D. M. Wood. 2000. "A kinematic hardening constitutive model for natural clays with loss of structure." *Géotechnique* 50 (2): 153–164. https://doi.org/10.1680/geot.2000.50.2.153.

Rowe, P. W. 1962. "The stress-dilatancy relation for static equilibrium of an assembly of particles in contact." *Proc. R. Soc. London, Ser. A* 269 (1339): 500–527. https://doi.org/10.1098/rspa.1962.0193.

Simith, P. R., R. J. Jordine, and D. W. Hight. 1992. "The yielding of bothkennar clay." *Géotechnique* 42 (2): 257–274. https://doi.org/10.1680/geot.1992.42.2.257.

Stipho, A. S. A. 1978. "Experimental and theoretical investigation of the behavior of anisotropically consolidated kaolin." Ph.D. thesis, Univ. of Wales, England.

Whittle, A. J. 1993. "Evaluation of a constitutive model for overconsolidated clays." *Géotechnique* 43 (2): 289–313. https://doi.org/10.1680/geot.1993.43.2.289.

Wood, D. M. 1990. *Soil behaviour and critical state soil mechanics*. Cambridge, UK: Cambridge University Press.

Wood, D. M., and J. Graham. 1990. "Anisotropic elasticity and yielding of a natural plastic clay." *Int. J. Plast.* 6 (4): 377–388. https://doi.org/10.1016/0749-6419(90)90009-4.

Yao, Y. P., Z. W. Gao, J. D. Zhao, and Z. Wan. 2012. "Modified UH model: Constitutive modeling of overconsolidated clays based on a parabolic Hvorslev envelope." *J. Geotech. Geoenviron. Eng.* 138 (7): 860–868. https://doi.org/10.1061/(ASCE)GT.1943-5606.0000649.

Yao, Y. P., W. Hou, and A. N. Zhou. 2008a. "Constitutive model for overconsolidated clays." *Sci. China Ser. E: Technol. Sci.* 51 (2): 179–191. https://doi.org/10.1007/s11431-008-0011-2.

Yao, Y. P., W. Hou, and A. N. Zhou. 2009. "UH model: Three-dimensional unified hardening model for overconsolidated clays." *Géotechnique* 59 (5): 451–469. https://doi.org/10.1680/geot.2007.00029.

Yao, Y. P., and Y. X. Kong. 2012. "Extended UH model: Three-dimensional unified hardening model for anisotropic clays." *J. Eng. Mech.* 138 (7): 853–866. https://doi.org/10.1061/(ASCE)EM.1943-7889.0000397.

Yao, Y. P., D. A. Sun, and H. Matsuoka. 2008b. "A unified constitutive model for both clay and sand with hardening parameter independent on stress path." *Comput. Geotech.* 35 (2): 210–222. https://doi.org/10.1016/j.compgeo.2007.04.003.

Yao, Y. P., and N. D. Wang. 2014. "Transformed stress method for generalizing soil constitutive models." *J. Eng. Mech.* 140 (3): 614–629. https://doi.org/10.1061/(ASCE)EM.1943-7889.0000685.

Zervoyanis, C. 1982. "Etude synth!etique des propri!et!es m!ecaniques des argiles et des sables sur chemin oedom!etrique et triaxial de revolution." [In French.] Ph.D. thesis, Central Institute of Technology of Paris, France.